

# A Feasibility Study for Active Remote Sensing of Atmospheric Carbon Monoxide Based on Differential Absorption of Infrared Radiation Along Vertical Paths

Fabrizio Cuccoli, Luca Facheris, Dino Giuli, *Senior Member, IEEE*, and Simone Tanelli, *Student Member, IEEE*

**Abstract**—In this paper, we describe a differential method for estimating mean concentrations of atmospheric molecular components along a quasivertical rectilinear Earth–air path utilizing a transmitter–receiver pair operating at infrared. The choice of a differential method is due to the need to limit calibration problems without utilizing more complex and costly systems such as DIAL, whose capabilities are definitely oversized for this kind of measurement. For this objective, a preliminary selection of the optimal wavenumbers for each molecular species of interest is needed. This is the main issue discussed in this paper, after which the analysis focuses on the effects of the uncertainties on atmospheric parameters that need to be estimated to provide the final mean concentration estimates. The feasibility study is carried out on carbon monoxide, considered as test species of interest in the reported simulations of atmospheric propagation, based on standard atmospheric models. Technological requirements are finally discussed.

**Index Terms**—Active remote sensing, carbon monoxide, infrared radiation, spectral attenuation measurements.

## I. INTRODUCTION

ATMOSPHERE-related quantities and parameters are typically obtained by spaceborne and airborne passive instruments like infrared/microwave radiometers and interferometric instrumentations [1]. The increasing use of satellites pushes the research toward the realization of systems, based both on spaceborne/airborne and ground instrumentation, designed to exploit attenuation measurements at the infrared [2], [3]. However, these systems suffer from an intrinsic lack of accuracy mainly caused by uncertainties about the emissivity function (temperature profile, source emissivity, etc.). Radiometers suffer also from a basic spatial resolution problem (related to their standard field of view) that does not allow for local scale measurements over areas of particular interest (for instance over urban areas or natural gas emission zones).

In this paper, we analyze an active infrared measurement system, not necessarily alternative to passive systems, since it may provide complementary information for estimating the total amount of atmospheric components along a quasivertical Earth–air/space measurement path. The system offers a better opportunity for monitoring phenomena that develop themselves in limited areas, thanks to a spatial resolution (defined by the

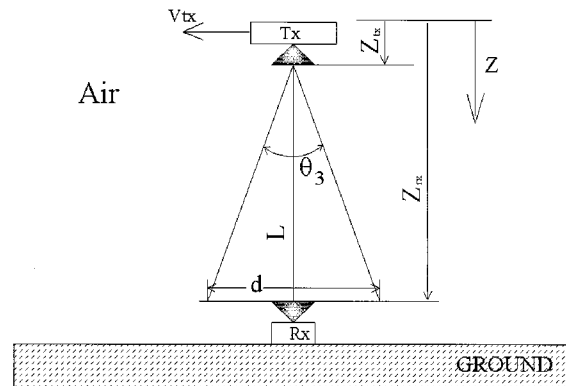


Fig. 1. Simple scheme of an atmospheric transmitter-receiver pair.

transmitter–receiver link) higher than that provided by passive instruments.

Though the system analysis presented in the paper has a general theoretical validity and holds for any monitored molecular species, we focus on the case of carbon monoxide for two reasons. First, this is to provide the reader with a clear example useful for understanding the approach used, and second, because CO is an atmospheric component of paramount interest in the remote sensing of the atmosphere. Applications of this technique are foreseeable in the remote sensing of atmospheric pollutants by airborne/spaceborne sensors, in particular over areas of interest such as volcanic areas, plants, and densely inhabited urban zones.

The paper is structured as follows. In Section II, the basic principles of infrared propagation in the atmosphere are reviewed. This section introduces the differential attenuation method discussed in Section III, exploited for estimating the amount of molecular components by means of power measurements from which link attenuations are obtained. In Section IV, we discuss more in depth the power/system requirements posed by the proposed application, in different operative modes. Finally, Sections V and VI deal with the CO case, exploiting a standard atmospheric model and a spectroscopic data compilation.

## II. ATTENUATION OF INFRARED RADIATION IN THE ATMOSPHERE

Let us consider a transmitter–receiver pair, as sketched in Fig. 1,  $z_t$  and  $z_r$  being the transmitter and receiver positions, respectively. The spectral radiance received in  $z_t$  can be expressed

Manuscript received December 3, 1999; revised February 24, 2000. This work has been supported by the Italian Space Agency, Ispra, Italy.

The authors are with the Dipartimento di Ingegneria Elettronica, Università di Firenze, 50139 Firenze, Italy.

Publisher Item Identifier S 0196-2892(01)00985-8.

using the formal solution of the one-dimensional (1-D) radiative transfer [4]

$$J(z_r, \nu) = J(z_t, \nu) e^{-\tau(z_t, z_r, \nu)} + \int_{z_t}^{z_r} S(z, \nu) e^{-\tau(z, z_r, \nu)} dz \quad (1)$$

where

- $\nu$  wavenumber in  $\text{cm}^{-1}$ ;
- $J(z_t, \nu)$  spectral radiance incident upon  $z_t$ ;
- $S(z, \nu)$  accounts for the spectral emission contributions between  $z$  and  $z + dz$  along the integration path;
- $\tau(z_1, z_2, \nu)$  so-called optical depth corresponding to a path length ( $z_2 - z_1$ ), and it is defined by the relation

$$\tau(z_1, z_2, \nu) = \int_{z_1}^{z_2} k(z, \nu) dz \quad (2)$$

where  $k(z, \nu)$  (dimension  $[L^{-1}]$ ) is the extinction coefficient of the propagation medium. It accounts for the power losses between  $z$  and  $z + dz$ .

For the limiting case, where the first term of (1) is much greater than the second one (namely, when the transmitted spectral radiance is much greater than the emission contributions  $S(z, \nu)$ ) and considering the emission from a point source, we obtain the Beer-Lambert law in terms of the spectral irradiance  $I(z, \nu)$

$$I(z_r, \nu) = I(z_t, \nu) e^{-\tau(z_t, z_r, \nu)}. \quad (3)$$

The natural logarithm of the total attenuation  $A(\nu)$ , defined as the ratio between transmitted and received irradiance, is the optical depth. Thus

$$A(\nu) = e^{\tau(z_t, z_r, \nu)}. \quad (4)$$

The attenuation coefficient  $k(z, \nu)$  depends on several different contributions that can be decomposed in Rayleigh, Mie, and molecular absorption, respectively, denoted as  $k_R$ ,  $k_M$ , and  $k_G$  [5].  $k_G$  accounts for all the absorbing molecular species along the integration path. Thus,  $k(z, \nu)$  can be expressed as the sum of all separate contributions

$$k(z, \nu) = k_R(z, \nu) + k_M(z, \nu) + \sum_{i=1}^N k_{Gi}(z, \nu). \quad (5)$$

$k_{Gi}(z, \nu)$  is related to the absorption of the  $i$ th molecular species between  $z$  and  $z + dz$  at the wave number  $\nu$ . This is generally given as the product between the concentration of the  $i$ th molecular species  $N_i(z)$  and its absorption cross section  $\sigma_i(z, \nu)$ . Such a section is then given as the sum of all absorption lines of the  $i$ th molecular species

$$\sigma_i(z, \nu) = \sum_l \sigma_{il}(z, \nu). \quad (6)$$

In the infrared range, the absorption lines  $\sigma_{il}$  are due to the vibro-rotational transitions, and their shape depends on atmospheric conditions, namely, pressure  $P$  and temperature  $T$ , so

the dependence of  $\sigma_i$  on  $z$  implies dependence on  $T(z)$  and  $P(z)$ . The optical depth of (2) can finally be decomposed as

$$\tau(\nu) = \tau_M(\nu) + \tau_R(\nu) + \sum_{i=1}^N \int_{z_t}^{z_r} N_i(z) \sigma_i(z, \nu) dz \quad (7)$$

where  $\tau_R$  and  $\tau_M$  are the optical depths related to  $k_R$  and  $k_M$ , respectively.

### III. DIFFERENTIAL ABSORPTION METHOD

Let us define  $\tau_0(\nu)$  as the optical depth due to a molecular species of which we want to measure the mean concentration over the integration path. The power  $P(\nu)$  collected using a receiver located in  $z_r$  is obtained by combining (3) and (7), yielding

$$P(\nu) = C I_t(\nu) \exp\{-[\tau_M(\nu) + \tau_R(\nu) + \tau_G(\nu) + \tau_0(\nu)]\} \quad (8)$$

where  $\tau_G(\nu)$  is related to the attenuation of all remainder molecular species,  $I_t(\nu) = I(z_t, \nu)$ , and  $C$  takes into account for the overall system losses (i.e., propagation attenuation, receiver characteristics).

Considering the transmission at two frequencies  $\nu_1$  and  $\nu_2$ , the power received at both frequencies is

$$P(\nu_1) = C_1 I_t(\nu_1) \exp\{-[\tau_M(\nu_1) + \tau_R(\nu_1) + \tau_G(\nu_1) + \tau_0(\nu_1)]\} \quad (9)$$

$$P(\nu_2) = C_2 I_t(\nu_2) \exp\{-[\tau_M(\nu_2) + \tau_R(\nu_2) + \tau_G(\nu_2) + \tau_0(\nu_2)]\}. \quad (10)$$

The ratio between these two received powers is then given by

$$\ln \left[ \frac{P(\nu_2)}{P(\nu_1)} \right] = \ln \left[ \frac{C_2 I_t(\nu_2)}{C_1 I_t(\nu_1)} \right] + [\tau_M(\nu_1) - \tau_M(\nu_2) + \tau_R(\nu_1) - \tau_R(\nu_2) + \tau_G(\nu_1) - \tau_G(\nu_2) + \tau_0(\nu_1) - \tau_0(\nu_2)]. \quad (11)$$

If  $\nu_1$  and  $\nu_2$  are such that

- 1)  $C_2 I_t(\nu_2) \cong C_1 I_t(\nu_1)$ ;
- 2)  $\tau_R(\nu_1) \cong \tau_R(\nu_2)$  and  $\tau_M(\nu_1) \cong \tau_M(\nu_2)$  (Rayleigh and Mie scattering effects are approximately the same at  $\nu_1$  and  $\nu_2$ );
- 3)  $\tau_0(\nu_1) \gg \tau_0(\nu_2)$  (the species of interest absorbs significantly more at  $\nu_1$  than at  $\nu_2$ );
- 4)  $\tau_0(\nu_1) \gg \tau_G(\nu_1)$  and  $\tau_0(\nu_1) \gg \tau_G(\nu_2)$  (the species of interest absorbs significantly more than all others at  $\nu_1$  and  $\nu_2$ )

the latter equation can be approximated, yielding

$$\ln \left[ \frac{P(\nu_2)}{P(\nu_1)} \right] \cong \tau_0(\nu_1). \quad (12)$$

Using (2) for  $\tau_0(\nu_1)$  and expressing the attenuation coefficient as the product between the concentration and the cross section, we obtain

$$\ln \left[ \frac{P(\nu_2)}{P(\nu_1)} \right] \cong \int_{z_t}^{z_r} N_0(z) \sigma_0(\nu_1, z) dz. \quad (13)$$

As mentioned above, the absorption cross section depends on temperature and pressure. As a consequence, when atmospheric propagation paths are not horizontal, the shape of  $\sigma_0$  depends on the altitude. Thus, it cannot be extracted from the integral.

Let us define an equivalent cross section  $\sigma_{eq}(\nu)$  such that

$$N_{mref}\sigma_{eq}(\nu)L = \tau_{0ref}(\nu) \quad (14)$$

where  $L = (z_r - z_t)$ ,  $\tau_{0ref}(\nu)$  is the optical depth referring to a predefined reference atmospheric model, and  $N_{mref}$  is the mean concentration over the integration path for the same reference model, namely,  $N_{mref} = (1/L) \int_{z_t}^{z_r} N_{0ref}(z) dz$ .

Indicating with  $N_m$  the mean concentration over the integration path, if  $\nu_1$  is such that

$$N_m\sigma_{eq}(\nu_1)L = \int_{z_t}^{z_r} N_0(z)\sigma_0(\nu_1, z) dz \quad (15)$$

holds for any possible plausible atmospheric condition (in terms of temperature and pressure profiles) or at any possible plausible concentration profile  $N_0(z)$ , we may rewrite (13) as

$$\ln \left[ \frac{P(\nu_2)}{P(\nu_1)} \right] \cong N_m L \sigma_{eq}(\nu_1). \quad (16)$$

In this way, one can obtain the mean concentration of a molecular species over a rectilinear path of length  $L$  through two power measurements carried out at two different wavelengths that satisfy the conditions 1–4 above. Of such conditions, the first two are mainly related to the transmitter's and receiver's characteristics (emitted power, optical efficiency, etc.). Concerning the remaining two conditions, the most severe is certainly the last one, since it requires a detailed analysis of spectroscopic characteristics of the species of interest.

#### IV. LINK DESIGN

In this section, referring to Fig. 1, we address the problem of designing the infrared transmitter-receiver system parameters based on their relative distance and velocity. Referring to a cylindrical coordinate system with the  $z$ -axis perpendicular to ground and the origin in the transmitter, the irradiance at the receiver (at distance  $L$  from transmitter) is

$$I_r(L, \rho) = \frac{P_0}{4\pi L^2} G(L, \rho) \frac{1}{A} \quad [\text{W/cm}^2] \quad (17)$$

where

- $P_0$  transmission power (Watt);
- $A$  total path attenuation;
- $G(z, \rho)$  gain pattern.

In the case of a Gaussian beam

$$G(z, \rho) = \frac{8}{\theta_3^2} e^{-2\rho^2/(z\theta_3)^2} \quad (18)$$

where  $\theta_3$  is the half power beamwidth. Assuming that the transmitter flies along a line parallel to the Earth with velocity  $V_t$ , the available illumination time (accounting for the half power beam only)  $t_{av}$  is

$$t_{av} = \frac{2L}{V_t} \text{tg} \left( \frac{\theta_3}{2} \right) \approx \frac{L\theta_3}{V_t}. \quad (19)$$

During  $t_{av}$ , attenuation measurements at the attenuated and reference wavenumbers  $\nu_1$  and  $\nu_2$  must be made. We shall assume that during  $t_{av}$ , two identical pulse signals of equal duration are transmitted at the two wavelengths. However, it must be recalled that the minimum integration time  $\tau_d$  of the infrared receiver is assigned depending on SNR requirements. In fact, in practice,  $\tau_d = 1/2\Delta f$ , where  $\Delta f$  is the receiver's noise bandwidth. Therefore, two cases can occur in general: 1)  $t_{av}$  fits the minimum signal to noise ratio requirements at the receiver ( $t_{av} > 2\tau_d$ , since two wavelength measurements are needed), and 2)  $t_{av} < 2\tau_d$ .

In the case of infrared receivers, the minimum received power can be written as a function of the detectivity  $D^*$  [4]

$$(P_{rx})_{\min} = \frac{SNR_{\min}}{D^*} (A_d \Delta f)^{1/2} \quad (20)$$

where  $A_d$  is the detector area (in  $\text{cm}^2$ ) and  $SNR_{\min}$  is the minimum acceptable SNR. The minimum received power is obtained by (17) assuming maximum attenuation  $A_{\max}$ . Therefore, combining (17) and (20) we get

$$\frac{SNR_{\min}}{D^*} (A_d \Delta f)^{1/2} = \frac{P_0}{4\pi L^2} \frac{8}{\theta_3^2} \frac{1}{A_{\max}} A_d \quad (21)$$

from which

$$\frac{P_0 A_d^{1/2}}{\theta_3^2} = \frac{SNR_{\min}}{D^*} (\Delta f)^{1/2} \frac{4\pi L^2}{8} A_{\max}. \quad (22)$$

Typical receiver system parameters' values taken as reference in this kind of infrared remote sensing applications are  $D^* = 10^{11} \text{ Hz}^{1/2}/\text{W}$ ,  $SNR_{\min} = 2$  and  $\Delta f = 1 \text{ Hz}$  [13]. Notice that imposing  $\Delta f = 1 \text{ Hz}$  implies that a minimum value for  $\tau_d$  is imposed. Substituting such values in (22), one gets

$$\frac{P_0 A_d^{1/2}}{\theta_3^2} = \frac{\pi L^2}{10^{11}} A_{\max}. \quad (23)$$

The left term of (23) encompasses all system parameters that can be adjusted in the link design. For this reason, such terms will be estimated in the different operating cases discussed in the following.

As a final remark, notice that the transmitter and receiver roles can be exchanged without modifying the results, assuming a reciprocal propagation medium.

##### A. Spaceborne Case

For the spaceborne case, realistic parameters are  $L = 220 \text{ km}$ ,  $V_t = 7.5 \text{ km/s}$  (Shuttle). Having assigned a specific value to  $\Delta f$ , (19) gives a minimum value for  $\theta_3$ :  $(\theta_3)_{\min} = 35 \cdot 10^{-3} \text{ rad}$ . Thus, (23) becomes

$$P_0 A_d^{1/2} = 18.62 \cdot A_{\max} [w \cdot \text{cm}]. \quad (24)$$

##### B. Airborne Case

For the airborne case, we consider  $L = 10 \text{ km}$ , and  $V_t = 800 \text{ km/h}$ . Using the same value for the noise bandwidth  $(\theta_3)_{\min} = 22 \cdot 10^{-3} \text{ rad}$  and (23) gives

$$P_0 A_d^{1/2} = 0.015 \cdot A_{\max} [w \cdot \text{cm}]. \quad (25)$$

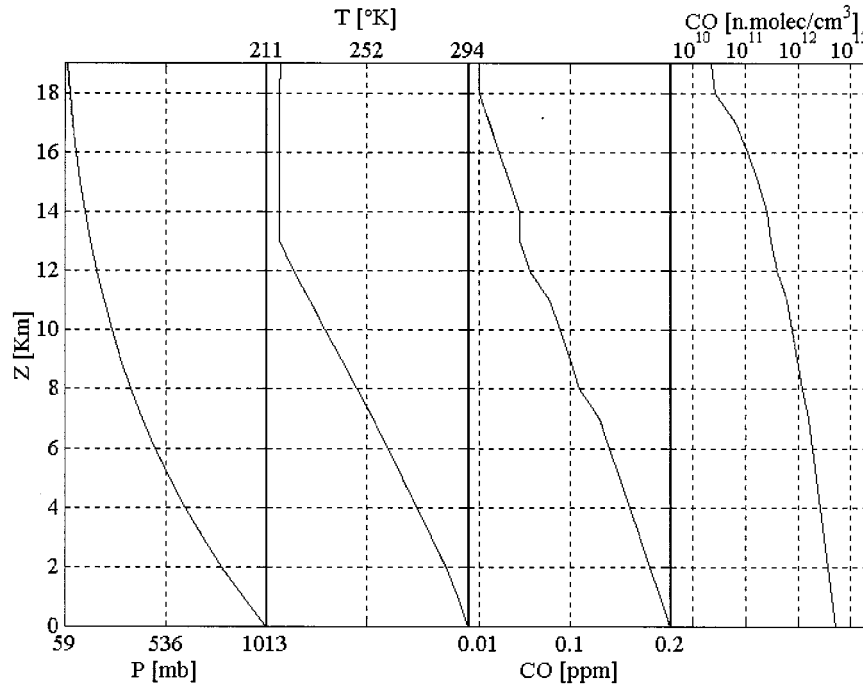


Fig. 2. Vertical profiles of temperature and pressure (standard summer atmosphere) and of CO concentration from ground to 20 km.

### C. Aerostat Case

In the aerostat case we choose  $L = 10$  km. In this case we assume that  $V_t = 0$ , in order to have no limitation about the detection time, the minimum for  $\theta_3$  depends exclusively by the transmitter's pointing system. We chose  $(\theta_3)_{\min} = 2 \times 10^{-3}$  rad (value obtainable by several off-axis paraboloids)

$$P_0 A_d^{1/2} = 1.26 \cdot 10^{-4} A_{\max}[w \cdot \text{cm}]. \quad (26)$$

As a final remark to the link design, it must be pointed out that scattering and Mie effects, increasing the propagation loss, cause in general a degradation of the SNR at the receiver. Unfortunately, any estimate of such additional attenuation would be extremely unreliable, since scattering and Mie effects are strongly dependent on regional characteristics of aerosols [6]. For this reason, they were not considered throughout this work. On the other hand, recent accurate studies on atmospheric transmission modeling allow to conclude that a signal degradation not exceeding 5% is expected caused by aerosols in the spectral region of interest (around  $4.7 \mu\text{m}$ , as indicated in the following sections) [7].

## V. ATTENUATION MEASUREMENTS IN THE SPECTRAL ABSORPTION INTERVAL OF CARBON MONOXIDE

The use of (16) to estimate the vertical amount of CO in the atmosphere through the differential attenuation method requires the preliminary determination of the two wavenumbers,  $\nu_1$  and  $\nu_2$ . The procedure adopted is based on spectroscopic data provided by the HITRAN96 database [8] and on standard models of atmosphere (molecular composition [9] profiles and temperature/pressure vertical profiles [10]). We computed the optical depth  $\tau_0 + \tau_G$  considering two spectral ranges. The first, around

$2169 \text{ cm}^{-1}$ , is characterized by the R6 CO absorption line [11], and the second, around  $2500 \text{ cm}^{-1}$ , is characterized by low molecular absorption. The vertical profiles of CO concentration, temperature and pressure are shown in Fig. 2.

Fig. 3 shows the attenuation  $A(\nu)$  around  $2169 \text{ cm}^{-1}$  over a vertical path considering the atmospheric layers from ground to 20 km altitude. To calculate the molecular cross sections, we accounted for all the absorption lines of the most abundant isotopes (those labeled as 1 in the HITRAN compilation [12]) in the range  $(2158, 2190) \text{ cm}^{-1}$ . In this spectral range, the main absorbing molecules are  $\text{H}_2\text{O}$ ,  $\text{N}_2\text{O}$ , and  $\text{CO}_2$ . In order to compute their concentration values, we considered a standard atmospheric composition. Observe that when  $\nu_1$  is comprised in the range  $(2169.1, 2169.3) \text{ cm}^{-1}$ , the total attenuation  $A(\nu_1)$  is only due to CO, so we have  $\tau_0(\nu_1) \gg \tau_G(\nu_1)$ .

The spectral attenuation around  $2500 \text{ cm}^{-1}$  is shown in Fig. 4 considering the same integration path. All the absorption lines contained in the  $(2483, 2510) \text{ cm}^{-1}$  range were accounted for. The main absorbing molecules in such spectral range are  $\text{N}_2\text{O}$ ,  $\text{CH}_4$ ,  $\text{H}_2\text{O}$ , and  $\text{N}_2$ , while absorption due to CO is negligible. Furthermore, total molecular attenuation is much lower than that around  $2169 \text{ cm}^{-1}$  (about three orders of magnitude). Therefore, choosing  $\nu_2 = 2501 \text{ cm}^{-1}$  conditions 3 and 4 listed in Section III are met, namely,  $\tau_0(\nu_1) \gg \tau_0(\nu_2)$ ,  $\tau_0(\nu_1) \gg \tau_G(\nu_1)$ , and  $\tau_0(\nu_1) \gg \tau_G(\nu_2)$ .

In order to determine the wavenumber that minimizes the error in the approximation of (13)–(16), we analyzed the optical depth variations in the  $(2169, 2169.5) \text{ cm}^{-1}$  range using 200 simulated profiles of CO concentration. Fig. 5(a) reports the reference CO profile used in simulations. We generated 200 different CO profiles independently and randomly. For each profile and from ground to 10 km altitude, the CO concentration was set free to vary uniformly within two orders of magnitude around the reference value. In this way, we obtained CO profiles having

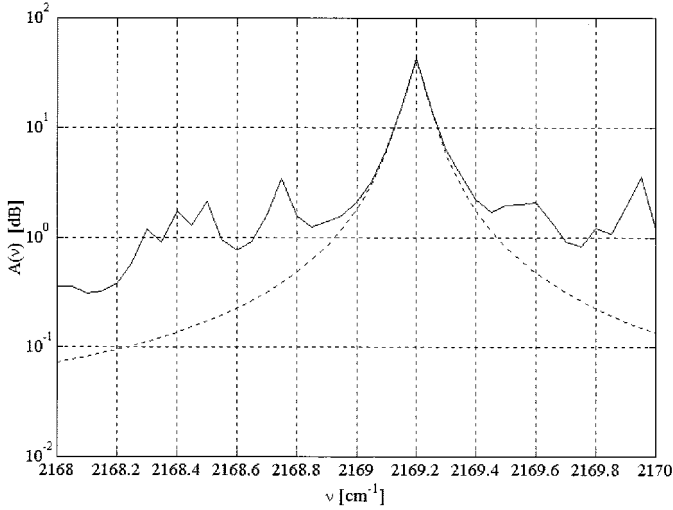


Fig. 3. Spectral attenuation around the R6 [11] absorbing CO line. Continuous line: total attenuation (mainly contributed by CO, CO<sub>2</sub>, N<sub>2</sub>O, and H<sub>2</sub>O); dashed line: attenuation contributions due to CO only.

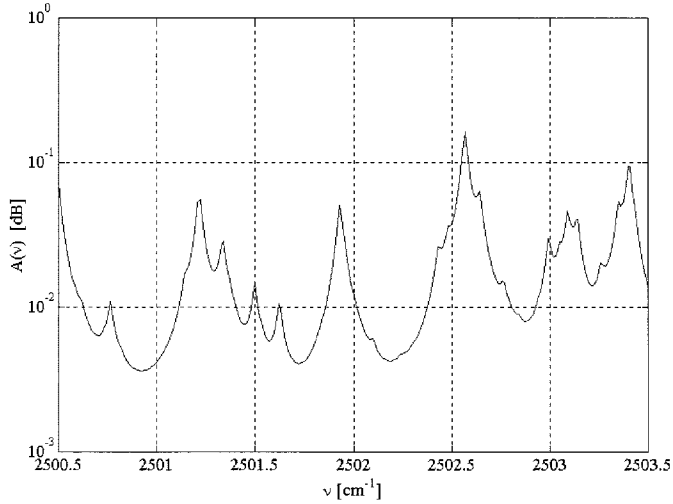


Fig. 4. Spectral attenuation around 2500 cm<sup>-1</sup>. Main contributors are H<sub>2</sub>O, N<sub>2</sub>O, CH<sub>4</sub>, and N<sub>2</sub>.

mean values, over a 20 km path length, ranging between about  $8.28 \cdot 10^{11}$  and  $6.48 \cdot 10^{12}$  molec./cm<sup>3</sup>.

Let us define the sensitivity absolute error  $es(\nu)$  as:

$$es(\nu) = \left| \frac{\tilde{\tau}_0(\nu) - \tau_0(\nu)}{\tau_0(\nu)} \right| \quad (27)$$

where  $\tau_0(\nu)$  is the “true” optical depth, and  $\tilde{\tau}_0(\nu)$  is the optical depth approximated using  $\sigma_{eq}(\nu)$ .  $\tilde{\tau}_0(\nu)$  is thus given by

$$\tilde{\tau}_0(\nu) = N_{om} \sigma_{eq}(\nu) L \quad (28)$$

where  $N_{om}$  is the mean concentration over the integration path of length  $L$ , relevant to a CO simulated concentration profile. The reference atmospheric model used to compute the equivalent cross section  $\sigma_{eq}(\nu)$  is that shown in Fig. 2. In Fig. 5(b) are plotted the variation bars (max and min values) of the spectral attenuation for the complete set of the 200 CO profiles. Finally, Fig. 5(c) shows the minimum and maximum values of  $es(\nu)$

for the same profiles. Notice that at 2169.15 cm<sup>-1</sup> and 2169.24 cm<sup>-1</sup>  $es(\nu)$  is smallest, assuming values around 5%. Moreover, at these two wavenumbers, the attenuation  $A(\nu)$  is extremely variable (some tens of dB).

## VI. EFFECTS OF VARIATIONS OF TEMPERATURE AND PRESSURE

The accuracy with which the mean concentration along the integration path can be estimated depends also on the vertical profiles of temperature and pressure and on their short term variations. In this section, we examine the effects of the uncertainty of such profiles on the mean concentration estimates. The approach used for this purpose is the same described in Section V for the variations of concentration. The error functional exploited is still that of (27), where  $\tau_o$  is the “true” optical depth computed by modifying the temperature and pressure profiles, while  $\tilde{\tau}_o$  is that computed using (28) (we recall that  $\sigma_{eq}$  is *always* computed by means of the standard profiles).

For each profile and from ground to 20 km altitude, temperature and pressure were set free to vary uniformly in an interval respectively equal to 5% of their reference value. Fig. 6 and Fig. 7 refer, respectively, to temperature and pressure (the profiles and their variation ranges are plotted in the upper left figure). They show that the effects of this kind of uncertainty are definitely negligible with respect to the effects of the uncertainty on the concentration profiles. In fact, in the temperature case and in the wavenumber region of interest, we get errors less than 0.5%, with the minimum errors occurring at the wavenumbers selected through the aforementioned method. In the pressure case, the error pattern is practically the same: the error is more than double, however at the selected wavenumbers we still get the minimum errors.

As mentioned in Section IV, the quantification of scattering and Mie effects would be extremely unreliable. It is, however, envisaged that the dependence on wavenumber of both  $\tau_R$  and  $\tau_M$  is such that the relative spectral distance, using  $\nu_1 = 2169.15$  (or 2169.4) and  $\nu_2 = 2501$ , is not sufficient to invalidate condition 2.

## VII. CONCLUSIONS

The proposed active method for estimating the total amount of atmospheric components is an alternative to passive infrared systems, bringing major advantages in those cases where high resolution and spatially localized monitoring is needed (volcanic areas, industrial plants, urban areas etc.). As far as technological requirements are concerned, as shown in the CO case, the power measurements that must be performed according to the proposed method require a spectral resolution better than 0.1 cm<sup>-1</sup>. This asks for infrared laser sources such as semiconductor diode lasers, largely employed for the measurement of molecular concentrations of atmospheric components along horizontal ground paths [13]. The main limitations are obviously encountered for the transmission power in the Earth-satellite case, for which peak powers of about 1 kW are needed to meet the minimum requirements discussed in case A of Section IV. Instead, power levels achievable by semiconductor transmission diodes [14] are sufficient to meet the requirements posed by cases B and C, assuming a reference

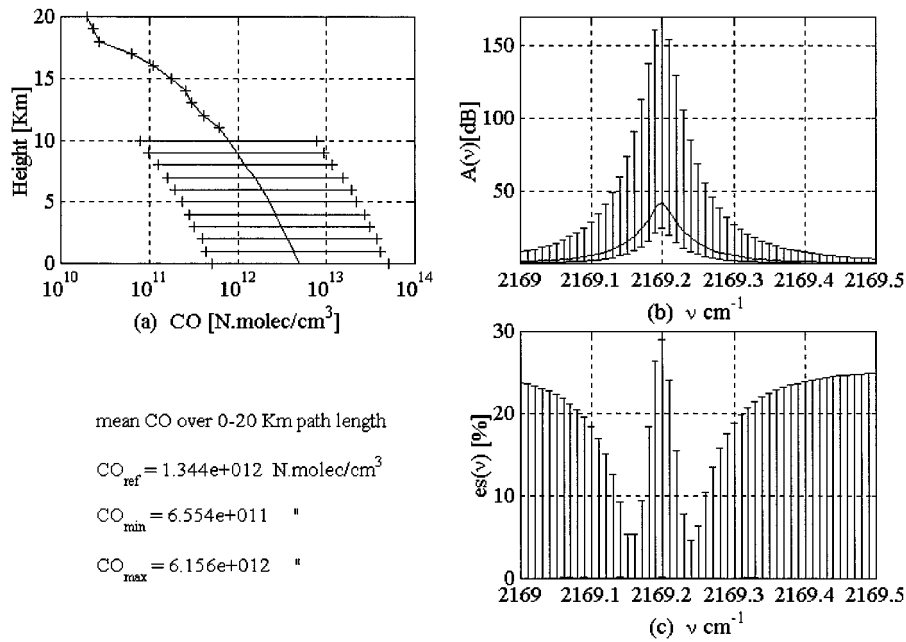


Fig. 5. (a) Reference CO vertical profile (continuous line) and variation ranges for the random generation of 200 profiles. (b) Spectral attenuation due to CO around 2169.2 cm<sup>-1</sup> and variation bars (min and max) obtained considering all of the 200 CO profiles. (c) Variation bars (min and max) of the absolute sensitivity error  $es(\nu)$ .

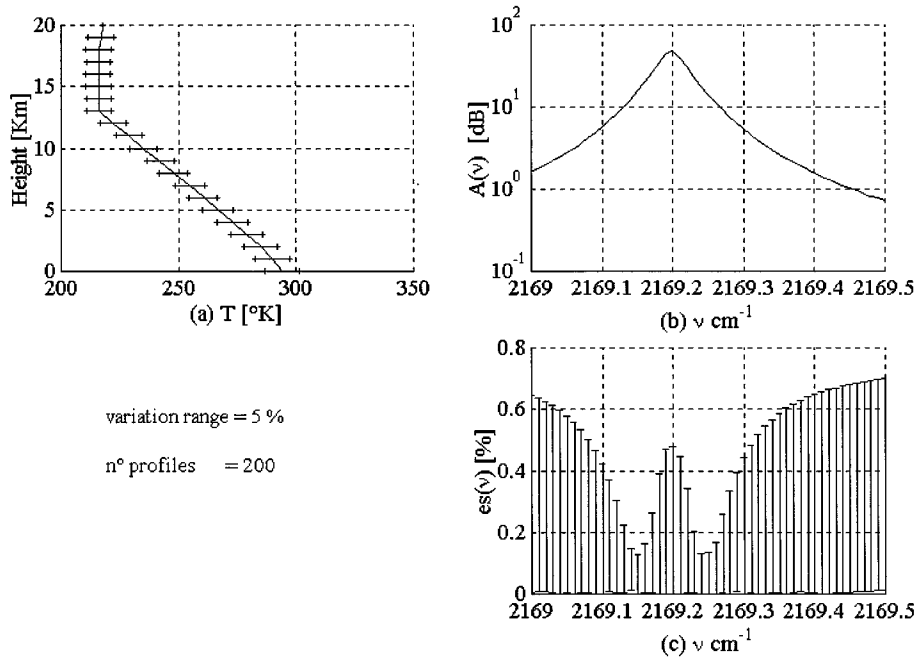


Fig. 6. (a) Reference temperature vertical profile (continuous line) and variation ranges for the random generation of 200 profiles. (b) Spectral attenuation due to CO around 2169.2 cm<sup>-1</sup> (pertinent to the CO reference profile). (c) Variation bars (min and max) of the absolute sensitivity error  $es(\nu)$ .

value of the order of 100 cm<sup>2</sup> for the equivalent area of the receiving optics and 20 dB maximum total attenuation.

The differential method for received power measurements, chosen so as to permit that spectral contributions that are "flat" in the frequency range within the two selected frequencies cancel each other on average, is sensitive only to time variations of the received power difference. Therefore, through a differential power stabilization system at the transmitter, measurements are directly exploitable without requiring *ad hoc* calibration. However, a residual calibration error is possible

caused by spatial inhomogeneities across the propagation beam (generated by turbulence effects in the atmosphere).

A foreseeable development of this matter concerns the reconstruction of two-dimensional (2-D) vertical concentration fields of atmospheric components by means of a tomographic network constituted by several quasivertical paths, built up by a single mobile transmitter and a baseline of receivers at ground. A tomographic approach to the reconstruction of 2-D horizontal fields of pollutants in limited areas was presented in [15]. Such an approach could be used for solving the cited vertical 2-D

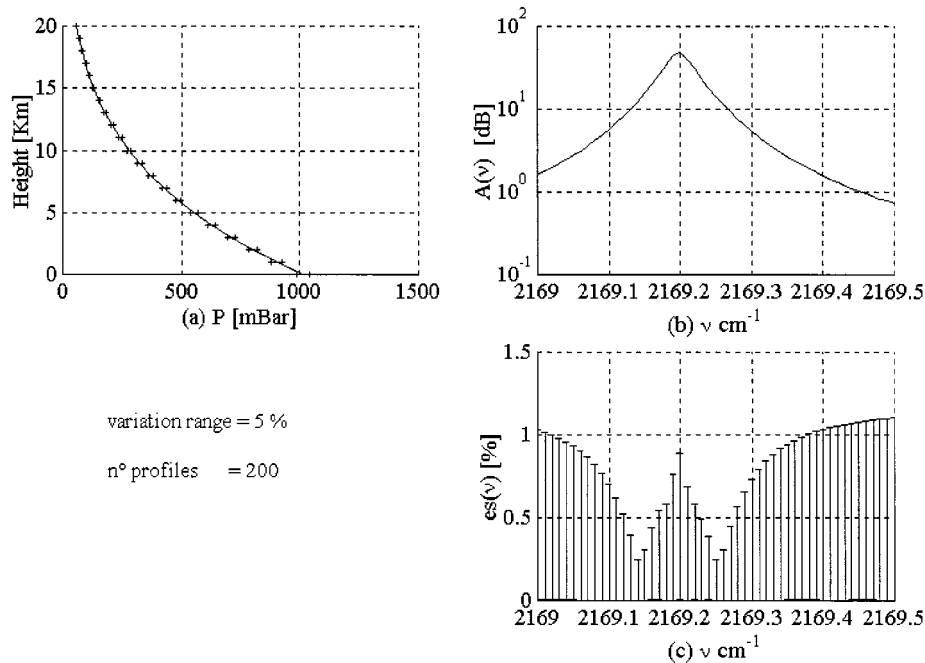


Fig. 7. Same as Fig. 6, referring to the pressure profile.

inversion problem. However, a specific redefinition of the algorithm reported there is required due to the intrinsic lack of vertical resolution of the mentioned 2-D vertical tomographic network.

#### ACKNOWLEDGMENT

The authors wish to thank L. Capannesi for his technical support.

#### REFERENCES

- [1] H. J. Kramer, *Observation of the Earth and Its Environment*. Berlin: Springer-Verlag, 1996.
- [2] "Retroreflector-in-space for ADEOS: Earth-space-Earth laser long-path absorption measurement of atmospheric trace species," in *Optical Remote Sensing of the Atmosphere, 1990 Technical Digest Series of the Optical Society of America*, vol. 4, pp. 488–490.
- [3] CRIEPI, Project Tech. Rep. IMG Mission Operation and Verification Committee, Mar. 30 1999.
- [4] R. M. Measures, *Laser Remote Sensing*. New York: Wiley Interscience, 1983.
- [5] E. D. Hinkley, "Laser monitoring of the atmosphere," in *Topics in Applied Physics*. New York: Springer-Verlag, 1976.
- [6] V. L. Okulov, Y. A. Rezunkov, N. V. Sidorovski, and A. N. Starchenko, "Characteristics features of aerosol scattering of repetitively-pulsed CO<sub>2</sub>-laser radiation in the atmosphere," *J. Opt. Technol.*, vol. 66, pp. 954–957, Nov. 1999.
- [7] Z. Wan and Z. L. Li, "A physics-based algorithm for retrieving land-surface emissivity and temperature from EOS/MODIS data," *IEEE Trans. Geosci. Remote Sensing*, vol. 35, pp. 980–996, July 1997.
- [8] L. S. Rothman *et al.*, "The 1996 HITRAN molecular spectroscopic database and HAWKS (HITRAN atmospheric workstation)," *J. Quant. Spectrosc. Radiat. Transf.*, vol. 60, pp. 665–710, Nov. 1998.
- [9] M. A. H. Smith, Compilation of atmospheric gas concentration profiles from 0 to 50 km, in NASA Tech. Memo. 83 289, Washington, DC, Mar. 1982.
- [10] R. A. McClatchey, R. W. Fenn, J. E. A. Selby, F. E. Volz, and J. S. Garing, Optical properties of the atmosphere, in Environ. Res. Papers, 411, AFCL-72-0497, Air Force Cambridge Res. Lab., Bedford, MA.
- [11] E. J. McCartney, *Absorption and Emission by Atmospheric Gases*. New York: Wiley Interscience, 1982.
- [12] L. S. Rothman, "AFGL trace gas compilation: 1982 version," *Appl. Opt.*, vol. 22, no. 11, pp. 1616–1625.
- [13] R. T. Ku, E. D. Hinkley, and J. O. Sample, "Long-path monitoring of atmospheric carbon monoxide with a tunable diode laser system," *Appl. Opt.*, vol. 14, no. 4, pp. 854–861, 1975.
- [14] P. Werle, "A review of recent advances in semiconductor laser based gas monitors," *Spectrochimica Acta, Part A54*, pp. 197–236, 1998.
- [15] F. Cuccoli, L. Facheris, S. Tanelli, and D. Giuli, "Infrared tomographic system for monitoring the two-dimensional distribution of atmospheric pollution over limited areas," *Trans. Geosci. Remote Sensing*, vol. 38, pp. 67–73, Jan. 2000.



**Fabrizio Cuccoli** received the "Laurea" (M.S.) degree (cum laude) in electronic engineering and the Ph.D. in methods and technologies for environmental monitoring from the University of Florence, Florence, Italy, in 1996 and 2000, respectively.



He is currently with the Radar and Radiocommunications Laboratory Group, Department of Electronic Engineering, University of Florence, as a Researcher of the Consorzio Nazionale Interuniversitario Telecomunicazioni (CNIT). His main research interests are in the area of remote sensing of rainfall and of the atmosphere through active and passive systems (e.g., spaceborne rain radars, infrared and microwave Earth-satellite links). His current interest is the microwave and infrared spectral analysis of absorption characteristics of the atmosphere components and related attenuation measurements data processing.

**Luca Facheris** received the "Laurea" (M.S.) degree (cum laude) in electronic engineering from the University of Florence, Florence, Italy, in 1989, and the Ph.D. degree in electronic and information engineering from the University of Padua, Padua, Italy, in 1993.

Since 1993 he has been an Assistant Professor in the area of telecommunications with the Department of Electronic Engineering, University of Florence. His main research interests are in the area of signal and data processing for active remote sensing, radar polarimetry, ground and spaceborne weather radars, and methods for the exploitation of attenuation measurements at microwaves and infrared for remote sensing of the atmosphere.



**Dino Giuli** (SM'84) received the "Laurea" (M.S.) degree (cum laude) in electronics engineering from the University of Pisa, Pisa, Italy, in 1970.

Since 1973, he has been a Faculty Member of the Department of Electronics, University of Florence, Florence, Italy, where he is now Full Professor. His research interests have mainly been devoted to experimental and theoretical research in the field of radar systems. He is also involved in research in digital communications and telecommunication networks. His radar research is devoted to optimum processing of dual-polarization radar signals and data, and to their integration with data from other spaceborne or ground based sensors.

Prof. Giuli is a member of the Italian Electrical Association (AEI).



**Simone Tanelli** (S'94) received the "Laurea" (M.S.) degree (cum laude) in electronic engineering and the Ph.D. in methods and technologies for environmental monitoring from the University of Florence, Florence, Italy, in 1995 and 1999, respectively.

He is currently with the Radar and Radiocommunications Laboratory Group, Department of Electronic Engineering, University of Florence, and with the Radar Science and Engineering Group, JPL/NASA, Pasadena, CA. His main research interests are in the area of remote sensing of atmosphere. In particular, his research interests include: tomographic inversion problems, spectral analysis of absorption measurements through atmosphere, and ground/spaceborne weather radar data processing.